

Widespread presence of shallow cusps in the surface-brightness profile of globular clusters

Enrico Vesperini

Department of Physics, Drexel University, Philadelphia, PA 19104, USA

`vesperin@physics.drexel.edu`

and

Michele Trenti

University of Colorado, CASA, Dept. of Astrophysical & Planetary Sciences, 389-UCB, Boulder, CO 80309, USA

`trenti@colorado.edu`

ABSTRACT

Surface brightness profiles of globular clusters with shallow central cusps ($\Sigma \sim R^\nu$ with $-0.3 \lesssim \nu \lesssim -0.05$) have been associated by several recent studies with the presence of a central intermediate mass black hole (IMBH). Such shallow slopes are observed in several globular clusters thanks to the high angular resolution of Hubble Space Telescope imaging. In this Letter we evaluate whether shallow cusps are a unique signature of a central IMBH by analyzing a sample of direct N-body simulations of star clusters with and without a central IMBH. We “observe” the simulations as if they were HST images. Shallow cusps are common in our simulation sample: star clusters without an IMBH have $\nu \gtrsim -0.3$ in the pre-core-collapse and core-collapse phases. Post-core-collapse clusters without an IMBH transition to steeper cusps, $-0.7 \lesssim \nu \lesssim -0.4$, only if the primordial binary fraction is very small, $f_{bin} < 3\%$, and if there are few stellar-mass black holes remaining. Otherwise ν values overlap the range usually ascribed to the presence of an IMBH throughout the entire duration of the simulations. In addition, measuring ν is intrinsically prone to significant uncertainty, therefore typical measurement errors may lead to $\nu \geq -0.3$ even when $\langle \nu \rangle \lesssim -0.4$. Overall our analysis shows that a shallow cusp is *not* an unequivocal signature of a central IMBH and casts serious doubts on the usefulness of measuring ν in the context of the hunt for IMBHs in globular clusters.

1. Introduction

Several observational studies have provided strong evidence for the presence of super-massive black holes with masses M_{BH} in the range $10^6 \lesssim M_{BH}/M_\odot \lesssim 10^9$ at the centers of elliptical and spiral galaxies. The masses of these central black holes correlate with the host-galaxy bulge mass and velocity dispersion (see e.g. Gültekin et al. 2009). If these correlations are extrapolated to smaller stellar systems, globular clusters should harbor intermediate-mass black holes (hereafter IMBHs) with masses in the range $10^2 - 10^4 M_\odot$.

Despite significant observational efforts, conclusive evidence of the presence of IMBHs in clusters is still lacking. Observational studies of Galactic clusters have so far provided only upper limits on the masses of IMBHs (see van der Marel & Anderson 2010 and references therein). The difficulty of obtaining an unambiguous detection is illustrated by the Omega Cen case. Based on integrated light spectroscopy from the ground and an HST-based surface brightness profile, Noyola *et al.* (2008) claimed a $4.0^{+0.75}_{-1.0} \times 10^4 M_\odot$ IMBH. However, proper-motion-velocity-dispersion data obtained with HST (van der Marel & Anderson, Anderson & van der Marel 2010) show that $M_{BH} \lesssim 1.8 \times 10^4 M_\odot$ (at 3σ confidence) in contrast with the Noyola *et al.* result. Outside the Milky Way, the presence of a central IMBH has been suggested for G1, a massive cluster in M31. Here radio, X-ray observations and dynamical studies all suggest the presence of an IMBH with $M_{BH} \sim 2 \times 10^4 M_\odot$ (Gebhardt *et al.* 2005, Ulvestad *et al.* 2007), but because of the limited spatial resolution of the observations (G1 is at about 800 Kpc, compared to the $\lesssim 10$ Kpc for many Galactic clusters), it is hard to probe the central region with proper motions or star-by-star radial velocities to evaluate the robustness of the G1 IMBH detection.

Given the difficulty of achieving a definitive detection of an IMBH, several studies have focused on possible signatures for its presence, both to construct circumstantial evidence based on a coincidence of indicators, as well as to identify a sample of promising candidates for detailed kinematic follow-up. In young clusters, X-ray (ULX) emission due to gas accretion is expected (see e.g. Miller & Colbert 2004). Dynamic signatures are related to the formation of a Bahcall-Wolf density cusp (Bahcall & Wolf 1976) within the sphere of influence of the BH. The three-dimensional density cusp induces a shallow cusp ($\Sigma \sim R^\nu$, with $-0.3 \lesssim \nu \lesssim -0.05$) in the projected surface brightness and velocity dispersion (Baumgardt *et al.* 2005, Trenti *et al.* 2007a, Miocchi 2007, Umbreit *et al.* 2009). In addition, these numerical studies showed that IMBHs can act as a very efficient energy source in clusters because of enhanced three-body interactions within the BH sphere of influence, supporting large cores and preventing core-collapse. Finally, Gill *et al.* (2008) have shown that the presence of an IMBH in a globular cluster can quench the process of mass segregation and introduced a new IMBH indicator based on the radial profile of the mean star mass within

a cluster. This indicator has been successfully applied to two globular clusters NGC2298 (Pasquato *et al.* 2009) and M10 (Beccari *et al.* 2010), ruling out a $M > 300 M_{\odot}$ IMBH (3σ confidence) in the first case and providing weaker limits in the second.

An important property for a reliable IMBH fingerprint is its uniqueness. For example, while systems in which a small core-to-half-mass radius ratio is observed are unlikely to host a IMBH, the converse is not necessarily true. Other dynamic processes, primarily two-body interactions of dark remnants with main sequence stars, provide efficient heating on the visible population of stars and may mask the development of core collapse (Trenti *et al.* 2010). Motivated by the recent attention given to the presence of shallow central cusps as fingerprints of IMBH in a number of observed Galactic and Magellanic Clouds clusters (see e.g. Noyola & Gebhardt 2006, 2007, Lanzoni *et al.* 2007), we discuss in this Letter the likelihood of observing shallow cusps in systems without an IMBH. For this, we take a set of direct N-body simulations of star clusters and analyze their surface-brightness profiles as we were ”observing” them with HST (see Trenti *et al.* 2010).

The outline of this Letter is the following. Section 2 summarizes the setup of our N-body simulations and defines the analysis tools we use. Section 3 presents the results on the time evolution of the central slope in the surface brightness profiles. In Section 4 we conclude with a discussion of our results in the context of IMBH searches.

2. Method and Initial Conditions

2.1. N-body simulations

The simulations considered here are a subset of those presented in Trenti *et al.* (2010). We summarize here the main ingredients of our numerical framework. Further details are provided in Trenti *et al.* (2010).

We follow the evolution of star clusters using the direct summation code NBODY6 (Aarseth 2003) run with its GPU extension on the NCSA Lincoln Cluster. The code models the effects of internal relaxation with an accurate treatment of the multiple interactions between stars obtained thanks to special regularization techniques.

The initial structure of the clusters is that of tidally limited King (1966) models. In the simulations presented here, the initial star masses are drawn either from a Miller & Scalo (1979) or a Salpeter (1955) initial mass function. Our analysis is focused on the late evolutionary stages of clusters as driven by two-body relaxation; before starting the run, we performed an instantaneous step of stellar evolution to evolve the mass function to a $0.8 M_{\odot}$

turnoff using the Hurley et al. (2000) evolutionary tracks. The evolution of the clusters has been followed until either $t = 8000$ (with the time expressed in N-body units, equivalent to the cluster dynamical time) was reached (corresponding to several initial relaxation times — $t > 16 t_{rh}(0)$) or at least 80% of the initial mass was lost due to evaporation of stars.

In order to explore the role of primordial hard binaries, our sample of simulations includes systems without primordial binaries as well as systems with an initial fraction of binaries $f_{bin} = N_b/N$ (where N_b is the number of binary stars) ranging from 0 to 0.1. The binaries’ binding energy distribution function is flat in log scale between ϵ_{min} and $133\epsilon_{min}$ where $\epsilon_{min} = \langle m(0) \rangle \sigma_c(0)^2$ where $\langle m(0) \rangle$ is the initial mean stellar mass and $\sigma_c(0)$ is the initial central velocity dispersion (see Trenti et al. 2007b, 2010).

In all the simulations we assumed that all the dark remnants produced are retained in the cluster; the comparison of the results of systems with a Miller-Scalo and a Salpeter initial mass function (which have a similar fraction of white dwarfs and neutron stars but produce a significantly different fraction of stellar-mass black holes: $\sim 1.5 \times 10^{-4}$ for Miller-Scalo and $\sim 1.4 \times 10^{-3}$ for Salpeter) allows us to explore the dependence of our results on the fraction of massive dark remnants. One simulation includes an IMBH with mass 1% of the total cluster mass.

The initial properties of the simulations considered here are summarized in Table 1, along with the identification used below to refer to them.

2.2. Data Analysis

In analysing the structural properties of our simulated clusters, we follow a procedure aimed at reproducing as closely as possible the steps performed in the analysis of observational data. We construct a synthetic observation by first ignoring all particles except main sequence stars. As our simulations only have an instantaneous step of stellar evolution, we do not consider stars along the giant branch. This choice is appropriate to create a surface brightness profile for main sequence stars. Focusing on main sequence stars leads to a significant reduction in the surface brightness profile fluctuations arising from the small number of luminous giants that would otherwise dominate the light profile. The mass difference between the upper main-sequence stars we used and the giants should have a negligible effect on the surface-brightness profile.

We then select a random direction, project the main-sequence stars’ positions and create a 2-dimensional map. A circular surface brightness profile, $\Sigma(R)$, is constructed using $2\text{Int}[\sqrt{N_{MS}}]$ annuli (where N_{MS} is the number of main sequence stars) each containing

$\sim \sqrt{N_{MS}}/2$ sources. The center of the system is determined by using the Casertano & Hut (1985) density-center method. We then determine the King concentration parameter $c = \log_{10}(r_t/r_c)$ by fitting the surface brightness profile with a single-mass King (1966) model (see Trenti et al. 2010 for further details on the construction of the surface brightness profile and the fitting procedure and for the time evolution of c).

This Letter is focused on the evolution of the inner part of the surface brightness profile. Specifically, we assume that in the inner parts $\Sigma(R) \propto R^\nu$ and estimate ν by a fit of $\Sigma(R)$ between the innermost $\Sigma(R)$ point (typically at 0.05-0.08 r_c) and $r_c/3$ (or using at least the three innermost points) where r_c is the King core radius for the best-fit King model. Previous simulations of clusters with an IMBH (Baumgardt et al. 2005) show that shallow cusps extend to about $r_c/3$. In order to estimate the range of values of ν obtained with this procedure when a cluster structure is that of a King model, we created 100 different random realizations of a King model with $W_0 = 7$ and 32K particles. After calculating the surface brightness profile for each system using the same number of annuli used in the data analysis of our simulations, we calculated ν for each random realization using data points within $r_c/3$. The mean value of ν obtained is ~ -0.05 with a dispersion of ~ 0.07 . Note that a small but non-zero value of ν for a King model is to be expected. This can be easily verified also by adopting the King (1962) analytical expression $\Sigma = \Sigma_o/(1 + (R/R_c)^2)$ to describe the inner surface density profile of a King model: fitting this analytical profile with a power-law between $\sim 0.05r_c$ and $r_c/3$ yields $\nu \sim -0.05$. Smaller values of ν might be obtained by restricting the radial range to regions closer to the center, but such an approach may be complicated by fluctuations in the surface brightness profile of a cluster’s innermost regions and, for actual data, possibly by the lack of adequate resolution.

Despite the different procedure adopted to measure the inner slope, our results are consistent within 1-sigma with the analysis of artificial images of King models discussed in Noyola & Gebhardt (2006; see e.g. their results for $N = 50000$ in the ‘subtracted’ and ‘10% subtracted’ panels of their Fig.4).

3. Results

The six panels of Fig. 1 show the time evolution of the index ν for the simulations with 32K particles. A smooth curve fit to the data has been added to highlight the evolutionary trend. The grey shaded area shows the range of values of ν expected for systems hosting IMBHs based on past studies (Baumgardt et al. 2005, Miocchi 2007). Our IMBH run falls within this range presenting a shallow inner cusp with slope $\nu \sim -0.25$, approximately constant during the entire cluster evolution.

The results of the simulation 32K (a system with no IMBH and no primordial binaries), on the other hand, show an evolution of ν characterized by three phases. For $t/t_{rh}(0) \lesssim 5$, the system is in the pre-core-collapse phase; as anticipated by our preliminary estimates of ν for a system described by a King model in §2, during this phase the value of ν undergoes significant fluctuations and, most of the time, falls in the range of values expected for systems hosting an IMBH (either directly or within 1-sigma).

The subsequent phase, $5 \lesssim t/t_{rh}(0) \lesssim 7$, is the core collapse phase and is characterized by a transition to steeper slopes typical of the post-core-collapse phase. During a significant portion of this phase the system is characterized by a central shallow cusp with values of ν in the range expected for systems with an IMBH. Finally for $t/t_{rh}(0) \gtrsim 7$ the system¹ is in the post-core-collapse phase and the slope of the inner cusp oscillates in the range $\sim -0.4 - -0.7$; these values are steeper than those predicted for clusters hosting an IMBH but even during this phase, as a consequence of fluctuations and measurement errors, ν may occasionally fall in the range of values expected for globular clusters hosting an IMBH.

For systems with primordial binaries, the middle and lower panels of Fig. 1 show that, for a fraction of primordial binaries $f_{bin} \gtrsim 0.03$, the typical values of ν overlap with the range of values of a system with an IMBH also for $t/t_{rh}(0) \gtrsim 7$ when the core is supported by the primordial binaries’ burning. This makes it impossible to distinguish whether the central shallow cusp is a consequence of the presence of an IMBH or of the presence of primordial binaries in the cluster core. We point out that the small f_{bin} adopted here is consistent with that determined observationally for a number of Galactic clusters (see e.g. Davis et al. 2008).

In Figure 2 we show the results of our simulations with 64K particles. Simulation 64K confirms the results of the lower resolution run (32K), although the larger number of particles leads to a smaller average error on the estimate of ν . In order to further illustrate the reduction in the error on ν for an increasing number of particles, we also show in Figure 2 a panel with the time evolution of ν obtained by combining two consecutive snapshots of the simulation 64K. The three phases in the evolution of ν described above are evident in both panels. Other than the smaller error on ν for larger N, our simulations do not show any dependence of the evolution of ν on N: for the 32K run the average ν is 0.08 with a 1σ spread equal to 0.17 for $t/t_{rh}(0) < 5$ while the average ν is 0.52 with a 1σ spread equal to 0.19 in the post-core-collapse phase ($7 < t/t_{rh}(0) < 16$). For the 64K run the average ν (1σ spread) is 0.11 (0.13) for $t/t_{rh}(0) < 5$, and 0.55 (0.13) for $7 < t/t_{rh}(0) < 16$.

¹Note that the values of $t/t_{rh}(0)$ that separates these three phases might differ for systems starting with a different initial concentration.

For simulation 64K, the difference between the measured value of ν and $\nu = -0.3$ (the lower limit of the range associated with the presence of an IMBH) is, in the post-core-collapse phase, smaller than 1σ 20% of the time. The smaller error on ν when consecutive snapshots are combined leads to a reduced fraction of post-core-collapse snapshots (10% of the time in this case) during which ν is within 1σ from the black hole range.

Simulation 64KW05 shows a similar time evolution of ν and the only difference is the delay in the onset of the core collapse phase, because of the lower initial concentration.

Simulation 64K5bin also confirms the results of the analogous lower resolution run (32K5bin).

Finally, the results of the simulation with a Salpeter initial mass function show that the amount of dark remnants in a cluster plays a key role in driving the cluster evolution and in determining the shape of its inner surface brightness profile. In particular our results confirm that the presence of dark remnants can significantly delay the onset of core collapse (see e.g. Merritt et al. 2004, Mackey et al. 2008, Trenti et al. 2010) and, in doing so, they extend the pre-core-collapse phase characterized by small values of ν consistent with those of systems hosting an IMBH. Dark remnants also play an important role in the post-core-collapse phase: specifically, by segregating in the cluster inner regions and heating the visible cluster population, dark remnants tend to produce a shallower core-collapse cusp than that observed in systems with no primordial binaries, no IMBH and a smaller population of dark remnants.

4. Discussion

Our simulations show that during their evolution, clusters without an IMBH are often characterized by central shallow cusps in the surface brightness profile with a slope falling in the range of values expected for systems with an IMBH.

For clusters in the post-core-collapse phase with neither primordial binaries nor a significant fraction of dark remnants, the inner cusp is steeper ($-0.7 \lesssim \nu \lesssim -0.4$) than that of systems with an IMBH. If we know that a cluster is in the post-core-collapse phase and has neither primordial binaries nor a significant fraction of dark remnants, then a shallow cusp in the range $-0.3 \lesssim \nu \lesssim -0.05$ could be indicative of an IMBH.

However, a small fraction of primordial binaries ($f_{bin} \gtrsim 0.03$) and/or the amount of dark remnants produced assuming a Salpeter stellar initial mass function (with a 100 per cent retention of dark remnants) act as a central heating mechanism sufficient to produce

a shallow inner cusp with the same range of slope values expected for systems hosting an IMBH.

Figure 3 summarizes the results of a representative subset of our simulations showing the different dynamical phases and cluster properties that can be associated with the presence of a shallow cusp. This figure nicely illustrates the problem faced by any attempt to use a shallow cusp as an indicator of the presence of an IMBH.

As an example, we plotted in Fig. 3 the Galactic clusters NGC 5694 and NGC 6388 for which Noyola & Gebhardt (2006) estimated, respectively, $\nu = -0.19 \pm 0.11$ and $\nu = -0.13 \pm 0.07$. Following Hurley (2007), we estimated the dynamical ages of NGC 5694 and NGC 6388 assuming $t_{rh}(0) \sim 2t_{rh}(now)$, where $t_{rh}(now)$ is the current value of the half-mass relaxation time (from the most recent version of the Harris(1996) catalogue)². The values for the slope of the inner cusp of these two clusters fall within the range of values expected for systems hosting an IMBH and indeed Umbreit et al. (2009) reproduced the NGC5694 surface brightness profile with a Monte Carlo simulation of a system hosting an IMBH with a mass $M_{BH} = 0.003 M_{cluster}$. As for NGC 6388, Lanzoni et al. (2007) fit the observed surface brightness profile with a multimass King model with an IMBH and suggested the presence of an IMBH with $M_{BH} \sim 5.7 \times 10^3 M_{\odot}$ ($\sim 0.0022 M_{cluster}$).

In Fig. 3 we show, however, that the slopes of the observed surface brightness profile of these clusters are also consistent with the results of simulations of systems without an IMBH under a variety of different initial conditions. In particular with the estimated dynamical age, these clusters might be either in the pre-core-collapse phase or currently entering the core-collapse phase. It is interesting to note that in a recent study based on radio observations of NGC 6388, Cseh et al. (2010) obtained an upper limit $M_{BH} < 735 \pm 244 M_{\odot}$, significantly smaller than the estimate of M_{BH} based on the surface density profile.

Our analysis clearly shows that shallow cusps in the surface brightness profile appear naturally during the dynamic evolution of star clusters without an IMBH. Therefore their presence in an observed profile cannot be used as a strong argument in favor of the presence of a central IMBH.

We acknowledge support from grants NASA-NNX08AH29G, NASA-NNX08AH15G, HST-AR-11284, TG-AST090094 and TG-AST090045.

²We emphasize that this dynamical age is very uncertain. Specific models for individual clusters (see e.g. Giersz & Heggie 2009) would be necessary for a higher accuracy determination of the cluster dynamical age.

REFERENCES

- Aarseth S., 2003, *Gravitational N-body Simulations*. Cambridge University Press
- Anderson, J., van der Marel, R.P., 2010, ApJ, 710, 1032
- Bahcall, J.N., Wolf, R.A., 1976, ApJ, 209, 214
- Baumgardt H., Makino J. and Hut, P. 2005, ApJ, 620, 238
- Beccari, G., Pasquato, M., De Marchi, G., Dalessandro, E., Trenti, M., Gill, M., 2010, ApJ, 713, 194
- Casertano S., Hut P., 1985, ApJ, 298, 80
- Cseh, D.; Kaaret, P.; Corbel, S.; Kording, E.; Coriat, M.; Tzioumis, A.; Lanzoni, B., 2010, MNRAS, 406, 1049
- Davis, D.S., et al., 2008, AJ, 135, 2155
- Gebhardt, K., Rich, R.M., Ho, L.C., 2005, ApJ, 634, 1093
- Giersz, M. and Heggie, D.C., 2009, MNRAS, 395, 1173
- Gill, M. et al. 2008, ApJ, 686, 303
- Gültekin, K. et al. , 2009, ApJ, 698, 198
- Harris, W. E., 1996, AJ, 112, 1487
- Hurley J. et al. 2000, MNRAS, 315, 543
- Hurley, J. 2007, MNRAS, 379, 93
- King, I. 1962, AJ, 67, 471
- King, I. 1966, AJ, 71, 64
- Lanzoni, B.; Dalessandro, E.; Ferraro, F. R.; Miocchi, P.; Valenti, E.; Rood, R. T., 2007, ApJ, 688, L139
- Mackey A. D., Wilkinson M. I., Davies M.B. and Gilmore G. F. 2008, MNRAS, 386, 65
- Merritt, D., Piatek, S., Portegies Zwart S. and Hemsendorf M. 2004, ApJ, 608, 25
- Miller, G. E. and Scalo J. E. 1979, ApJS, 41, 513

- Miller, M. C., Colbert, E. J. M., 2004, *IJMPD*, 13, 1
- Miocchi, P., 2007 MNRAS, 381, 103
- Noyola, E. and Gebhardt, K. 2006, AJ, 132, 447
- Noyola, E. and Gebhardt, K. 2007, AJ, 134, 912
- Noyola, E., Gebhardt, K and Bergmann, M., 2008, ApJ, 676, 1008
- Pasquato, M. et al. 2009, ApJ, 699, 1511
- Salpeter, E E. 1955, ApJ, 121, 161
- Trenti, M., Ardi, E. Mineshige, S. Hut, P. 2007a, MNRAS, 374, 857
- Trenti, M., Heggie, D. C and Hut, P. 2007b, MNRAS, 374, 344
- Trenti, M., Vesperini, E., Pasquato, M., 2010, ApJ, 708, 1598
- Ulvestad, J. S., Greene, J. E., Ho, L. C., 2007, ApJ, 661, L151
- Umbreit, S., Fregeau, J.M., Rasio, F.A., 2009, Submitted to ApJ
- van der Marel, R.P., Anderson, J., 2010, ApJ, 710, 1063

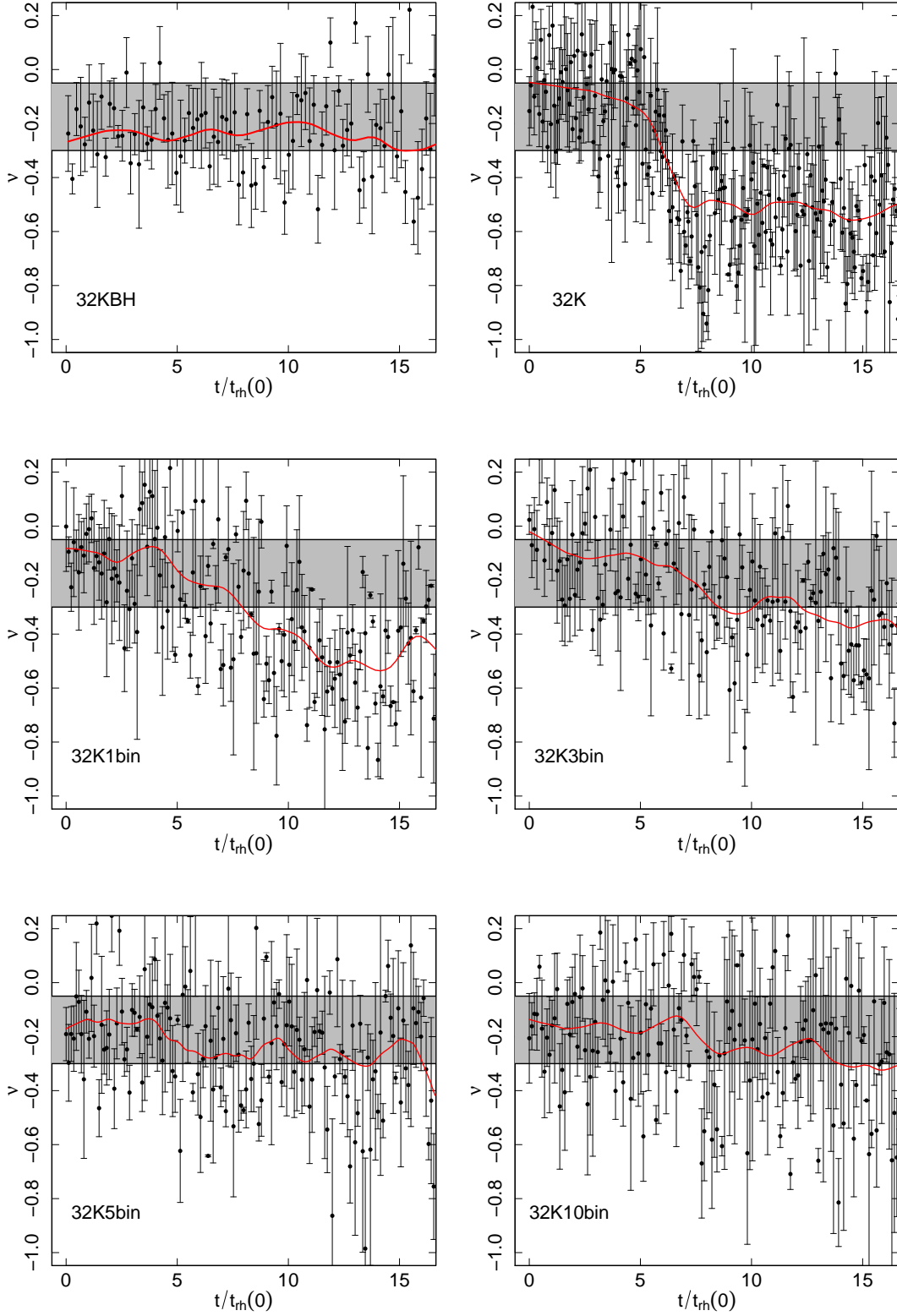


Fig. 1.— Time evolution of the slope, ν , of the inner surface brightness profile for the 32KBH (top left), 32K (top right), 32K1bin (middle left) and 32K3bin (middle right), 32K5bin (lower left), 32K10bin (lower right) simulations. The shaded area shows the range of values of ν expected for systems harboring an IMBH. The solid line in each panel show a smooth fit to the data.

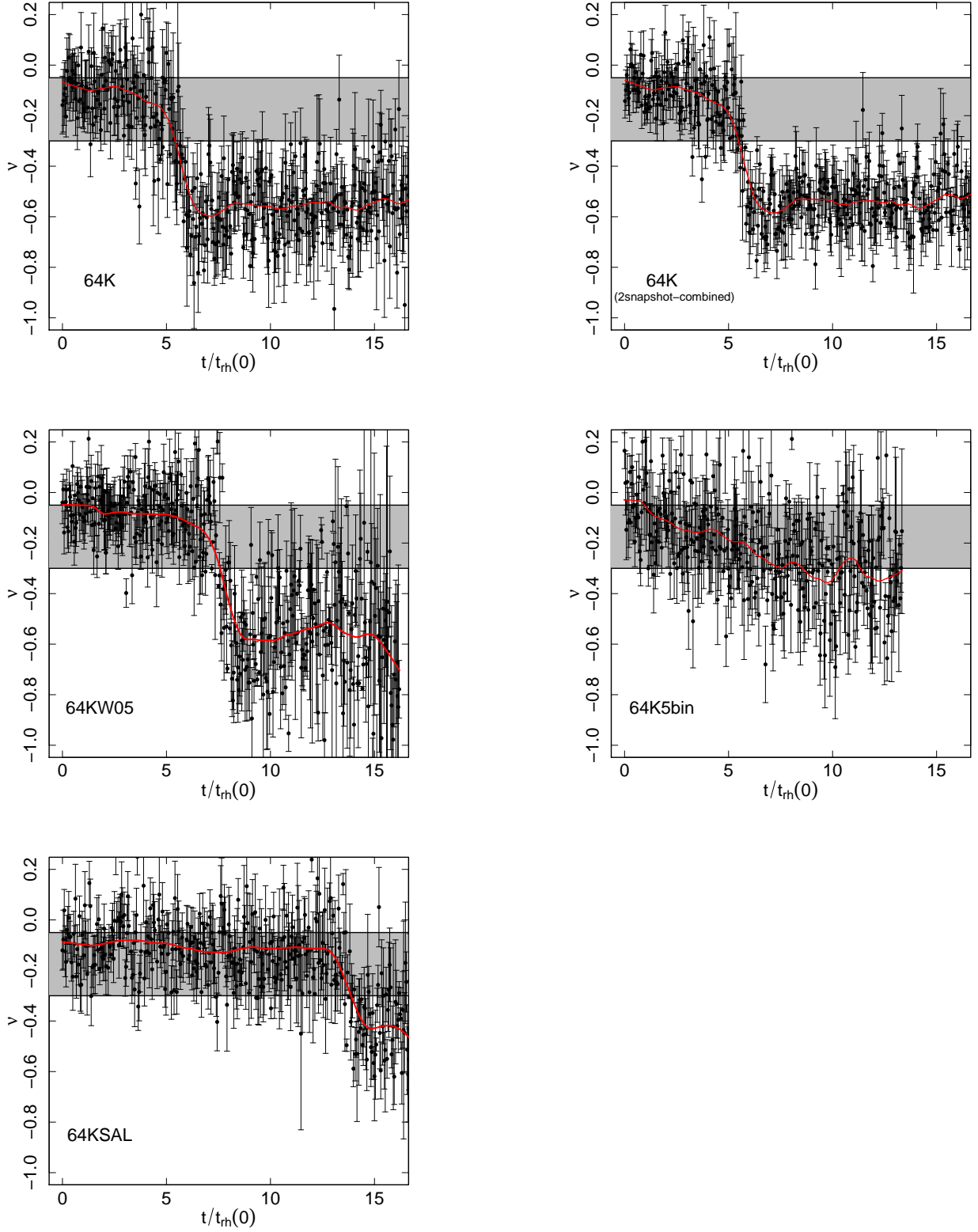


Fig. 2.— Shallow cusp slope ν versus time as in Figure 1 for runs: 64K (top left), 64K combining two consecutive snapshots (top right), 64KW05 (middle left), 64K5bin (middle right) and 64KSAL (lower left).

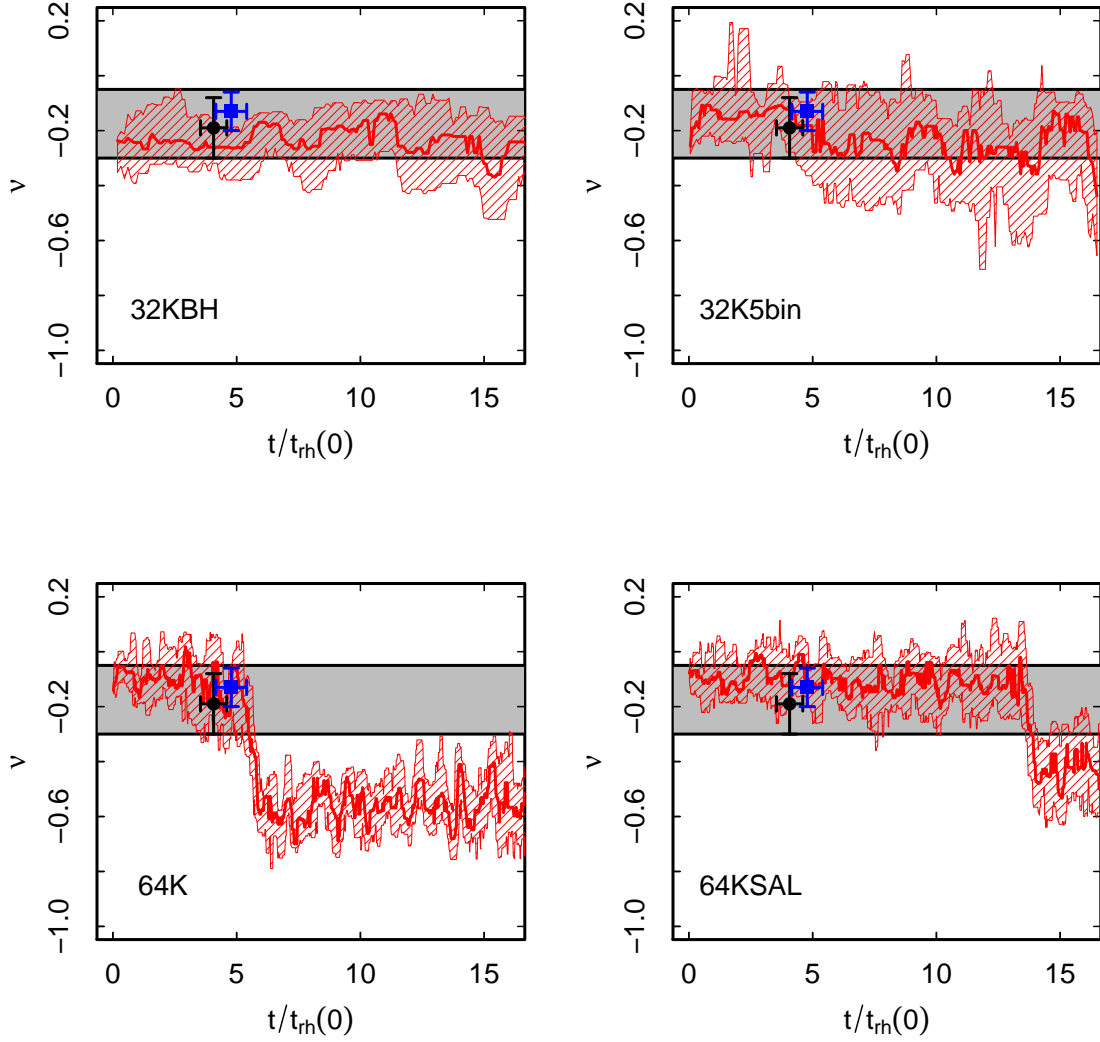


Fig. 3.— 1σ area of ν for the 32KBH (top left), 32K5bin (top right), 64K (bottom left), 64KSAL (bottom right). The upper (lower) line delimiting each shaded area represents the 84.1 (15.9) percentile of a moving bin including 15 values of ν . The dots show the slope of the inner cusp for NGC 6388 (filled blue square) and NGC 5694 (filled black dot) (values from Noyola & Gebhardt, 2006). The dynamical ages of these two clusters have been calculated assuming $t = 11.5 \text{ Gyr} \pm 1.5 \text{ Gyr}$ and $t_{rh}(0)$ has been calculated as $2t_{rh}$ where t_{rh} is the cluster current half-mass relaxation time (see section 4 for further discussion). The grey shaded area shows the range of values of ν expected for systems harboring an IMBH.

Table 1: Summary of N-body simulations

Id.	N	f_{bin}	IMF	W_0	$M_{BH}/M_{cluster}$
32KBH	32769	0.00	MS	7	0.01
32K	32768	0.00	MS	7	0.0
32K1bin	32768	0.01	MS	7	0.0
32K3bin	32768	0.03	MS	7	0.0
32K5bin	32768	0.05	MS	7	0.0
32K10bin	32768	0.10	MS	7	0.0
64KW05	65536	0.00	MS	5	0.0
64K	65536	0.00	MS	7	0.0
64K5bin	65536	0.05	MS	7	0.0
64KSAL	65536	0.00	Sa	7	0.0

Note. — Summary of initial conditions of the N-body simulations presented in this Letter. First column: Identification; second column: number of particles N ; third column: binary fraction $f_{bin} = N_b/N$; fourth column: initial mass function used (Sa: Salpeter, MS: Miller & Scalo); fifth column: initial concentration of the density profile (King index W_0); sixth column: IMBH mass in units of the total cluster initial mass.